Pure Appl. Chem., Vol. 71, No. 11, pp. 2067–2077, 1999.
Printed in Great Britain.

Optoelectronic processes in π-conjugated oligomers and polymers*

S. Barth, H. Bässler†, D. Hertel, V. I. Nikitenko and U. Wolf

Institut für Physikalische Chemie, Makromolekulare Chemie und Kernchemie und Zentrum für Materialwissenschaften, Philipps Universität, Hans-Meerwein-Str., D-35032 Marburg, Germany

Abstract: Based upon Monte-Carlo simulations, analytic theory, and experiment a hopping concept for charge injection into random organic π-functional dielectrics is been developed and tested. The treatment is flexible enough to include interfacial properties and to incorporate space charge limited current flow. A hopping concept has also been employed to analyse experimental data on the hole mobility in conjugated polymers. The time response of LEDs, though more complicated, can be rationalized in terms of self-consistent analytic theory. It has been applied to tunneling controlled time dependent electroluminescence in a bilayer LED.

INTRODUCTION

For a long time the desired property in regard to organic dye molecules was their colour and its functionality brought about by changing the length of the π-electron system. Meanwhile it has been recognized that the deliberate and easy manipulation of the energetic location of the highest molecular orbital (HOMO) as well as the lowest unoccupied molecular orbital (LUMO) by chemical tailoring opens up the door to a wide range of opto-electronic phenomena and which, traditionally, were associated with inorganic semiconductors only. Electrophotography is one of them. It exploits the charge transporting properties of π-conjugated molecules on a large industrial scale [1]. There are good reasons to suspect that other areas will develop similarly. Organic light-emitting diodes [2] may effectively compete with more traditional flat panel displays and photovoltaic cells and organic field transistors may follow. For application purposes one has, of course, to cope with the generic properties of organic systems and to take advantage of them, such as weak intermolecular bonding, low dielectric constant, and disorder. As a result, the mobilities of charge carriers are low as is the time response of devices, and the primary optical excitations are neutral implying that the efficiency of photogeneration is also quite modest. Further, given by the large bandgap, the equilibrium concentration of charge carriers in the bulk is very small and acceptor/donor doping is hard to achieve. The latter handicap can be circumvented by efficient charge injection from appropriate electrodes.

The purpose of this article is to develop a framework for charge carrier generation at a metallic or quasi-metallic electrode of an organic dielectric, such as a light-emitting diode (LED), to elaborate on carrier motion and, finally, to discuss selected aspects related to the temporal response of LEDs.

CHARGE CARRIER INJECTION

The classic treatment of charge carrier injection from a metal into a semiconductor is in terms of either Fowler-Nordheim (FN) tunneling or Richardson-Schottky (RS) thermionic emission [3]. In its original version, developed for inorganic crystalline semiconductors, the FN model ignores the coulombic potential. The RS model assumes that a carrier, once having acquired an energy sufficient to pass the

* Lecture presented at the 4th International Symposium on Functional Dyes—Science and Technology of π-Electron Systems, Osaka, Japan, 31 May–4 June 1999, pp. 2009–2160.
† *Corresponding author*: E-mail: baessler@mailer.uni-marburg.de

maximum of the superimposed image potential and the external potential, will not suffer inelastic back scattering. These are serious shortcomings, notably in a molecular solid in which transport occurs via short range hopping. For this reason we developed a formalism, both analytical as well as via Monte-Carlo simulation, to treat injection into a hopping system considering the long range coulombic potential as well as disorder [4,5].

The adopted model was an array of sites representing either a molecule in an organic glass or a segment of a conjugated polymer. Disorder was modelled in terms of a density of states (DOS) distribution of gaussian shape of variance σ. The initial injection event was realized in terms of an optimization procedure involving jumps from the Fermi level of the metallic electrode to interfacial states of the DOS followed by temperature and field assisted escape from the coulombic well next to the electrode. In the course of the simulation back scattering was automatically taken care of. Figure 1 shows the injection efficiency φ of charge carriers as a function of the electric field F and parametric in the zero field injection barrier Δ between the center of the DOS and the Fermi level. By separately counting injection events into the first and the second layer of the dielectric—this is a particular advantage of Monte-Carlo simulation—we could rule out that long range jumps are unimportant. This is an expected consequence of weak intersite coupling which is a characteristic feature of van-der-Waals bonded organic solids. It proves that FN tunneling is not the dominant injection process, notwithstanding the fact that $\ln j$ vs. F^{-1} plots approach a straight line behavior asymptotically, accidently yielding reasonable values for Δ, though. On the other hand, by plotting φ (F) data in the form appropriate for testing RS thermionic injection, it turns out that φ (F) does resemble a RS injection current, i.e.

$$j(F,T) = B\exp[-(\Delta-\beta F^{1/2})/kT], \tag{1}$$

where $\beta = [e/(4\pi\epsilon\epsilon_0)]^{1/2}$ and B is supposed to be given by AT^2 where $A = 60\ \mathrm{A/cm^2\,K^2}$ [3]. Equation 1 predicts that φ must saturate for $F > (\Delta/\beta)^2$ in accordance with Fig. 1. In quantitative terms there is a discrepancy. For $\epsilon = 3.5$, the theoretical value of the PF coefficient is $\beta = 2.0\times10^{-4}\ (\mathrm{V\dot{c}m})^{1/2}$ while simulation yields $\beta = 3.1\times10^{-4}\ (\mathrm{V\dot{c}m})^{1/2}$. Of even greater importance is the temperature dependence of $\varphi(T)$. Figure 2 shows, that on an Arrhenius scale $\varphi(T)$ plots are curved yielding significantly smaller values of the activation energy than the anticipated activation energy $\Delta - (eF/4\pi\epsilon\epsilon_0)^{1/2}$. This is known to be a signature of hopping motion in a gaussian shaped DOS. It is caused by (i) relaxation of hopping particles in the DOS and (ii) the transport energy being below the center of the DOS. This effect becomes more pronounced at lower temperatures [6].

In Fig. 3 a series of unipolar electron currents injected from a magnesium:silver cathode into a vapor deposited Alq_3 layer on top of a Al anode is presented on a RS scale [7]. The confirmation of a $\ln j$ vs. $F^{1/2}$ dependence is obvious, yielding a β coefficient which is about a factor of 2 larger than what RS theory would predict. Most gratifying, though, is that the temperature dependence matches the simulation result over three decades (Fig. 4). It turns out that an optimum fit is provided for $\Delta = 0.52\,\mathrm{eV}$. Considering the uncertainty of workfunctions and HOMO/LUMO levels the agreement with the expected value (0.7 eV) is good implying that any interfacial level off-set due to, for instance, a dipole layer must be <0.2 eV [8].

The comparison between simulation and experiment can be used to estimate the prefactor current which, according to RS theory, should be AT^2: The derivation of this expression is based upon the integration over momentum space for the thermally excited electrons implying that all momentum vectors inside the dielectric are allowed. In a hopping system this is not the case. By extrapolating the injection current towards $T\rightarrow\infty$ one arrives at the limiting current $j_\infty = 2.5\times10^4\ \mathrm{A/cm^2}$ a Mg:Ag electrode is able to deliver into an undiluted organic hopping system. Given this information one derives a criterion at which a given combination of injection barrier Δ and a charge carrier mobility would yield an electrode limited or a space charge limited (SCL) current [9]. Recall that an unipolar SCL current is the maximum current injected into a dielectric limited by the space charge built up by the moving charges [10]. Under this circumstance the electric field at the injecting electrode vanishes, the electrode being called ohmic. At constant charge carrier mobility μ and under the absence of trapping, the SCL current is given by Child's law, $j_{SCL} = 9/8\epsilon\epsilon_0\mu F^2/L$, L being the sample thickness. Thus, in order to establish SCL conditions, the injection current at zero field must exceed $j_{SCL}(F)$. Since the electrode limited and SCL currents depend on Δ and μ, respectively, one can establish a criterion concerning the injection barrier which can be tolerated at a given mobility (Fig. 5).

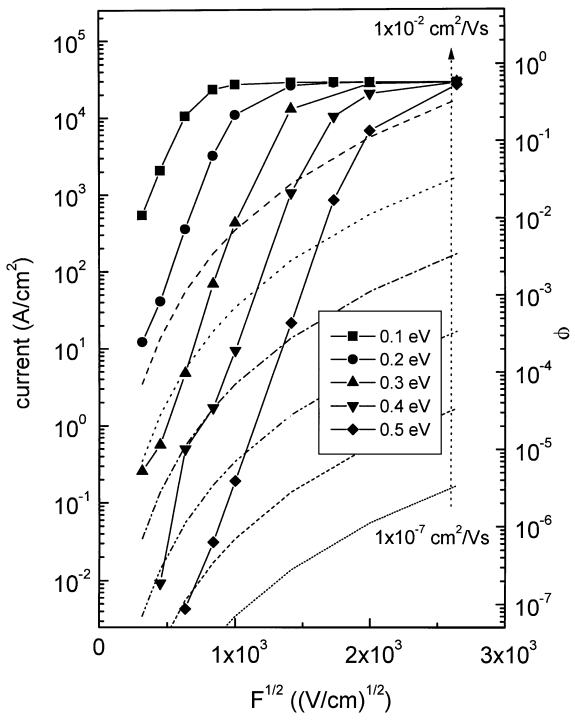

Fig. 1 Left scale: Injection efficiency from the Fermi level of a metal into a random organic dielectric as a function of the electric field F and parametric in the energy barrier Δ at $T = 295\,\mathrm{K}$ and $\sigma = 0.1\,\mathrm{eV}$. Right scale: Injection current calculated assuming $j_\infty = 2.5 \times 10^4\,\mathrm{A/cm^2}$. Dashed curves are the SCL currents according to Childs' law parametric in the carrier mobility.

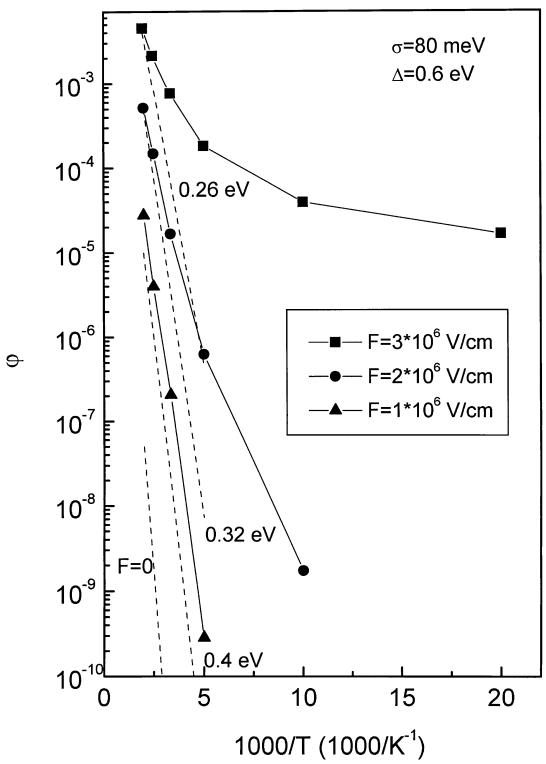

Fig. 2 Temperature dependence of the injection efficiency at different electric field. Dashed lines pertain to a system with no disorder and no back scattering of the carriers.

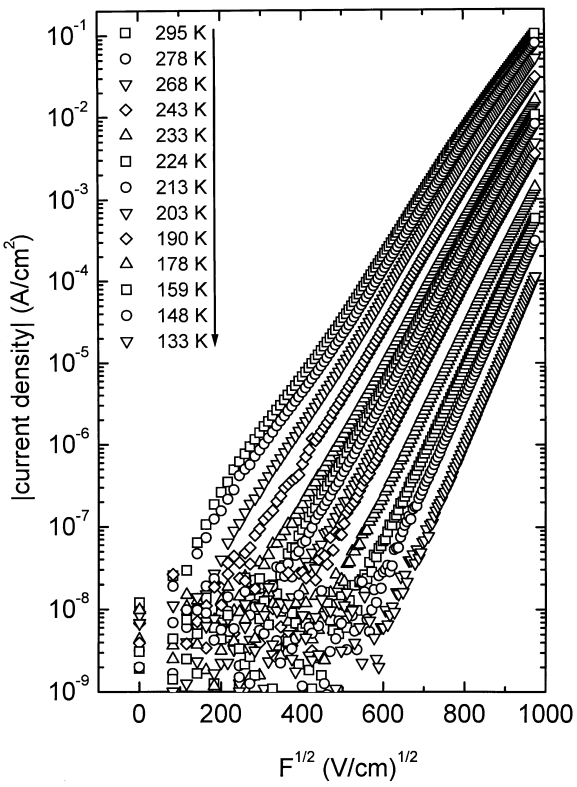

Fig. 3 $j(F)$ characteristics of an Al(+)|Alq_3 (150 nm)|Mg:Ag(–) device on lg j vs. $F^{1/2}$ representation. A built-in potential of 0.7 eV has been taken into account.

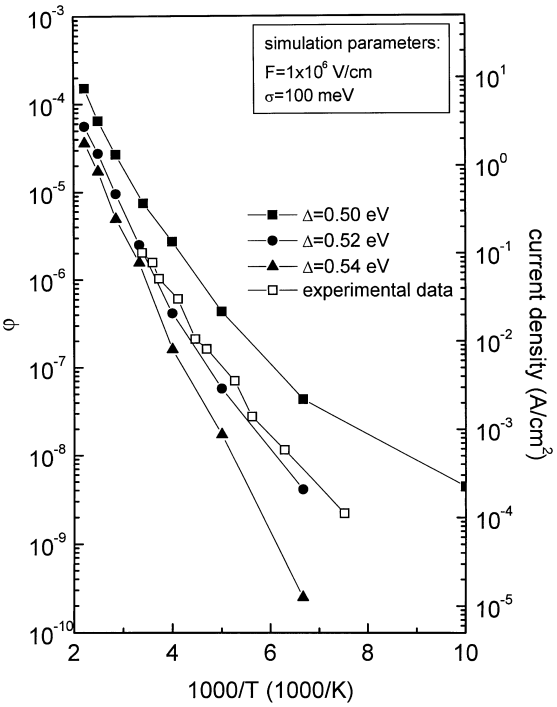

Fig. 4 The temperature dependence of the measured injection current at $F = 9.5 \times 10^5$ V/cm compared with the simulated injection efficiency for $\Delta = 0.50$ eV, 0.52 eV and 0.54 eV and $\sigma = 0.1$ eV.

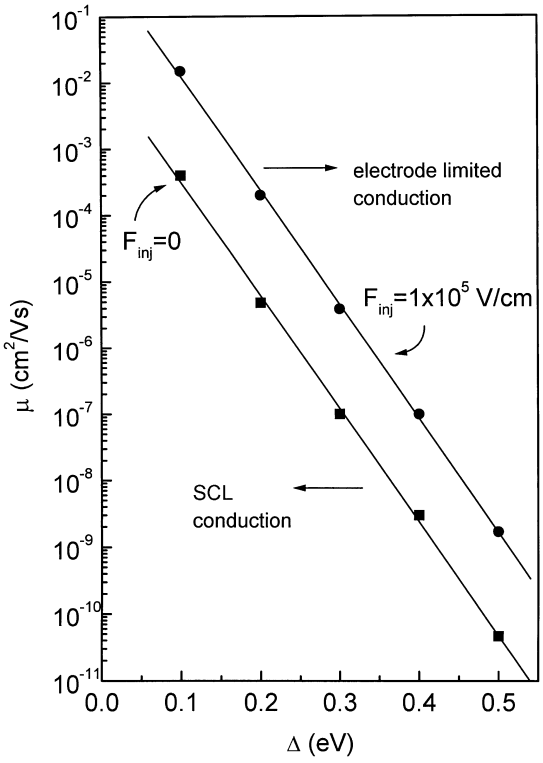

Fig. 5 Demarcation line separating the regimes of space charge limited unipolar conduction and electrode limited injection. The controlling parameters are the zero field energy barrier Δ and the carrier mobility, respectively.

The previous results pertain to ideal barriers between a metal electrode and a dielectric. In reality there may be inadvertant as well as deliberate surface effects. Aluminium is a notorious example. It may form an oxide or may react with PPV to form a covalently bound interfacial layer. Recently, it was found that electron injection from metals such as magnesium into LEDs can be enhanced by inserting a thin layer of an organic insulator such as lithiumfluoride [11]. One can propose a simple explanation of that effect based upon the recognition that the attenuation length of the electron wave function in a covalently or heteropolar inorganic insulator is much larger than in a van-der-Waals bonded organic solid. This is reflected by the different band width of inorganic and organic solids, for instance. From the dependence of the charge carrier mobility in a random organic solid as a function of the concentration of the transport sites it is known that the electronic coupling term $2\gamma a$ is of order 10 [12]. For a typical intersite distance of 0.6 nm, the wavefunction decay constant, γ^{-1}, is therefore about 0.12 nm. In amorphous silicon it is by a factor of 3 larger. In Al|AlO_2|Al tunneling devices the scattering length of an electron was found to be 1.2 nm. This is about one order of magnitude larger than in an organic glass. For that reason metal electrons can tunnel quite easily through a thin inorganic insulating layer. Moreover, target sites for the initial injection event into the first layer of the organic solid are further away from the metal. By this token they will start their subsequent random walk in the organic dielectric further away from the metal where the image potential is reduced. Therefore, also a greater proportion of the initially injected carriers can escape from the image potential and can be swept away by the collecting electric field.

The simulation results [14] presented in Fig. 6 confirm that injection is facilitated by a thin inorganic interfacial layer the more so when the energy barrier Δ increases. The effect is independent of other interfacial effects such as modification of the injection barrier due to a dipole layer. As the layer thickness increases the injection efficiency must—and does—decrease again because then tunnelling across the interfacial layer becomes rate limiting. The results of Jabbour *et al.* [15] on Mg:Ag|lithium fluoride|Alq_3 electrodes can, thus, be interpreted in simple terms.

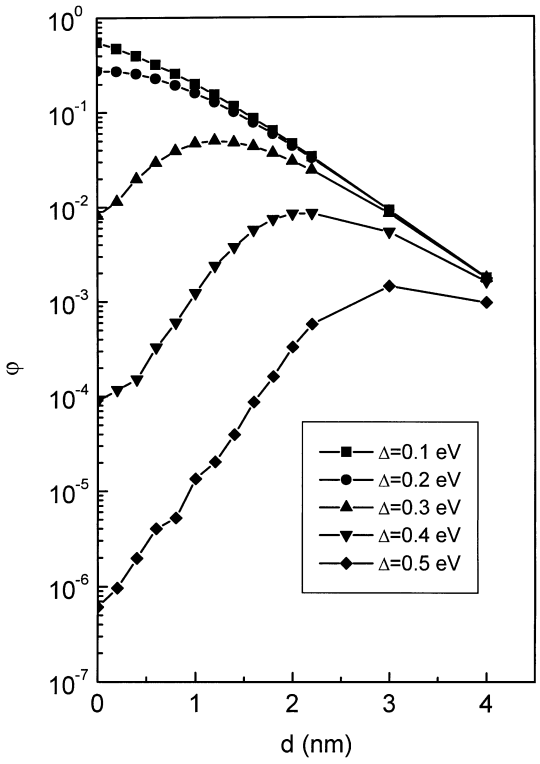

Fig. 6 Efficiency of charge injection from a metal into a random organic dielectric as a function of the thickness of an organic interfacial layer parametric in the zero field injection barrier Δ. ($T = 250$ K, $F = 1 \times 10^6$ V/cm, $\sigma = 80$ meV, $f = 0.1$).

CHARGE TRANSPORT IN CONJUGATED POLYMERS

The charge carrier mobility is one of the essential material parameters for an optoelectronic organic device, such as a LED. It determines how fast the reservoir of charge carriers required for electroluminescences to occur is established. As far as concepts is concerned it is straightforward to conjecture that the rate limiting step for macroscopic charge transport is intermolecular hopping among the manifold of sites acting as charge carrier entities. Therefore, charge carrier injection and transport should be considered to be complementary processes controlled by disorder and, concomitantly, by sample morphology, the classic experiment to probe charge transport being time of flight (TOF) technique [1].

From absorption and fluorescence spectroscopy it is known that conjugated polymers can be considered as an array of oligomers of statistical length manifested, for instance, by the inhomogeniously broadened optical band profiles [16]. It is straightforward to assume that radical cation and anion states, that is positively and negatively charged segments of a polymer, will form a corresponding distribution centered at a mean energy of the HOMO or LUMO. As far as low molecular organic glasses and molecular doped polymers is concerned, the phenomenology of charge transport has been rationalized in terms of a disorder model [17]. It is premised upon a gaussian distribution of localized states. One assumes that initially an ensemble of non-interacting charges, generated by injection or photoionization, will occupy hopping states randomly. After a while they tend to relax towards the tail states. Under the section of an applied field they will execute a field and temperature assisted hopping motion. There are several implications of this notion, for instance, the average energy of the hopping carrier decreases at lower temperatures. This should lead to a temperature dependent activation energy yielding an log μ vs. $(T_0/T)^2$ dependence where the characteristic temperature of the system is proportional to the variance of the gaussian distribution. Because an electric field must tilt the distribution the mobility must increase with field featuring a ln μ vs. $F^{1/2}$ law. The relaxation of the carriers must give rise to a decrease of the apparent carrier mobility at short times. At lower temperature this results in dispersive transport.

In this study two conjugated polymers were used to determine the hole mobility from TOF signals, a phenylamino substituted poly(phenylenevinylene) derivative (PAPPV) and a ladder-type methyl-substituted poly(para-phenylene) (MELPPP) [18]. Both differ concerning the degree of disorder as evidenced by the reduced inhomogenous broadening of MELPPP as compared to PAPPV, both in absorption and fluorescence (Figs 7, 8). TOF signals of PAPPV feature an ubiquitous pattern known from molecular doped polymers or organic glasses, i.e. there is an initial spike representing the initial relaxation of charge carriers towards quasi-equilibrium followed by a plateau and a broad tail. Below about 150 K the signals become dispersive and one has to determine the transit time from double logarithmic plots. For $T > 150$ K the temperature dependence of the hole mobility obeys a ln μ vs. T^{-2} law and from $\delta \ln \mu / \delta T^{-2}$ one arrives at a value $\sigma = 52$ meV for the variance of the DOS (Fig. 9). The break of the ln μ vs. T^{-2} dependence correlates with the onset of dispersive transport, the transition temperature being in accordance with previous simulation results. The predicted ln μ vs. $F^{1/2}$ dependence is also verified. Obviously, PAPPV behaves as the gaussian disorder model predicts.

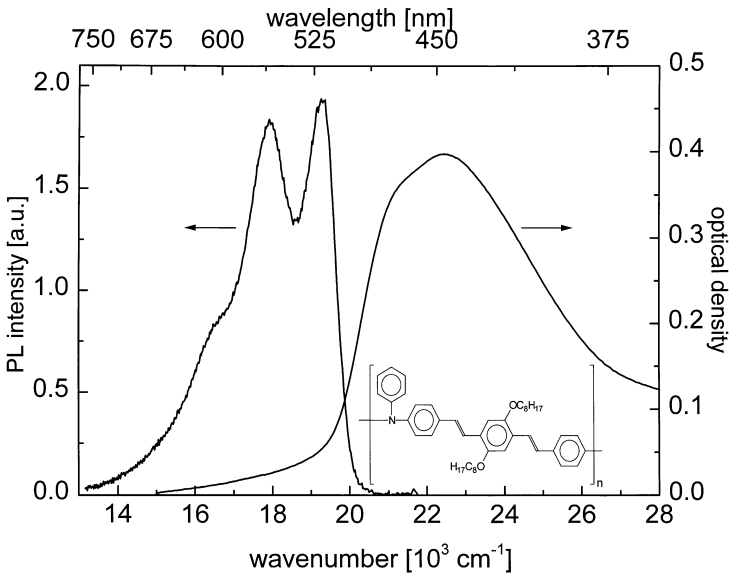

Fig. 7 Absorption and fluorescence spectra of a film of PAPPV at 295 K.

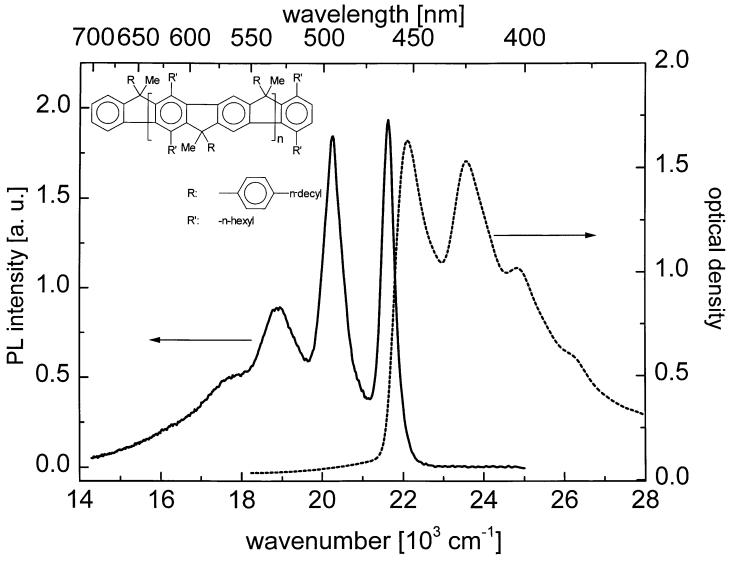

Fig. 8 Absorption and fluorescence spectra of a film of MeLPPP at 295 K.

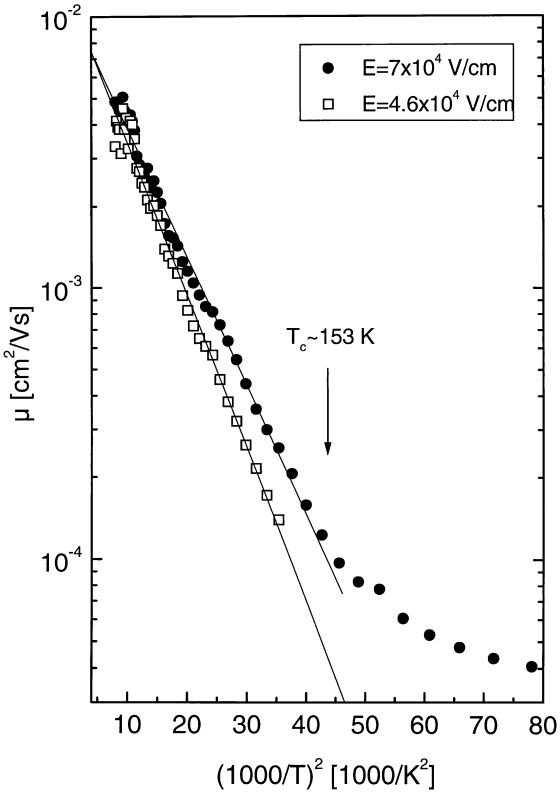

Fig. 9 The logarithm of the hole mobility in PAPPV vs. T^{-2}. The arrow marks the transition from nondispersive to dispersive transport.

The situation is different for MELPPP. The time of flight signal is almost that of a molecular crystal. The absolute mobility is of order $10^{-3}\,\mathrm{cm}^2/\mathrm{Vs}$ and, remarkably, the temperature dependence is very weak, not featuring a $\lg \mu$ vs. T^{-2} law. By plotting μ in terms of an Arrhenius law one arrives at an activation energy of order of 20 meV only. By the way, this means that trapping and polaronic effects are absent. Another noteworthy feature is that above 7×10^4 V/cm there is virtually no field dependence either (Fig. 10). Obviously these results cannot be interpreted in terms of the conventional disorder model. On the other hand, the mobility is 2–3 orders of magnitude less than in molecular crystals, such as anthracene or naphtalene [19]. Therefore the rate of charge transfer from one segment of a chain to another one must be several orders of magnitude less. Recall that from the variation of the absorption edge of oligomers as a function of their chain length yields to an effective conjugation length of about 6–7 nm [23]. Therefore, the step length per jump is one order of magnitude larger than the intermolecular separation among small molecules. It appears that improved order of the polymer is counterproductive for inter-chain hopping. By the way, a related phenomenon has been noted for crystalline polydiacetylene. While the onchain mobility of, presumable, electrons is around $5\,\mathrm{cm}^2/\mathrm{Vs}$ [20–22], the transverse mobility is 3–4 orders of magnitude less [24], i.e. $\mu \approx 10^{-3}\,\mathrm{cm}^2/\mathrm{Vs}$. This compares favourably to the $T \rightarrow \infty$ intercept of $\mu(T)$ of amorphous MELPPP which has to be controlled by inter-chain hopping. This suggests that charge delocalization reduces inter-chain coupling. Obviously more theoretical work is needed to elucidate inter-chain transport in such systems.

TRANSIENT ELECTROLUMINESCENCE

Applying a rectangular voltage pulse to an organic dielectric such as a LED yields information complementary to that of TOF studies. In principle, electroluminescence (EL) commences after a delay time t_d after the encounter of the fronts of electrons and holes [24]. In a single layer LED that time is given by the sum of the carrier mobilities, i.e. $t_d = L/[(\mu_+ + \mu_i)F]$. EL will saturate once the steady state concentrations of electrons and holes are established. Of greater interest is the case when space charges

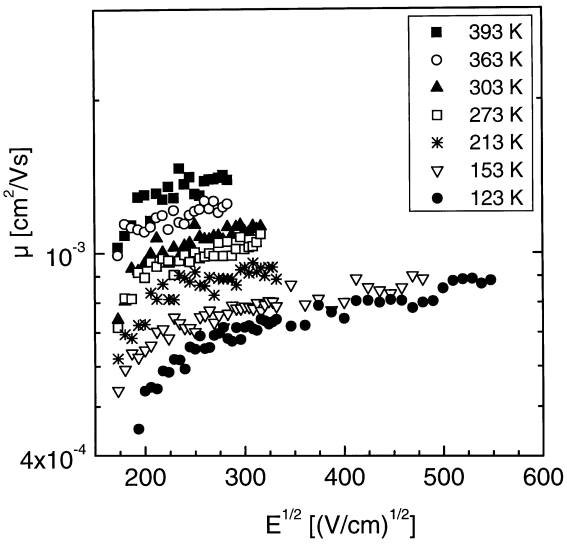

Fig. 10 The electric field dependence of the hole mobility in MeLPPP at different temperatures, plotted on a lg μ vs. $F^{1/2}$ scale.

accumulate at interfaces. Interfaces may be introduced deliberately in order to block carrier leakage [25] towards the electrodes and/or to spatially confine the recombination zone or they may be present inadvertantly, e.g. due to oxide formation at the cathode. Buildup of internal space charge will cause redistribution of the electric field inside the device and by this token must have a feedback effect on charge injection driving the LED towards balanced operation [26–28]. The rise behavior of EL will therefore be the result of a rather complicated interplay between injection, transport, space charge formation and recombination. In general, the delay time of EL exceeds the transit time of both the hole and electron transporting layers in bilayer diodes. The rise function is controlled by interfacial accumulation of majority carriers and the concomitant increase of the injection of minority carriers due to both the enhancement and screening of the electric field at the electrodes where minority and majority carriers are being delivered, respectively.

While in most cases the onset of EL occurs quite smoothly a rather abrupt turn-on has been observed [29]. In view of its potential technological importance this phenomenon will be discussed in some detail drawing heavily on the result of analytic theory [30]. The devices consisted in a tristilbeneamine (TSA) blended with polysulfone or an alkoxy-substituted PPV as an hole transporting layer combined with an electron transporting polystyrene copolymer carrying trifluoromethyl- or tert-butyl-substituted quaterphenyl pendant groups (CF_3–PQP). Upon addressing the LED by a rectangular voltage pulse the EL rises abruptly after a delay time and saturates almost instantaneously. The delay time increases with the time period between successive voltage pulses and decreases strongly with increasing electric field (Fig. 11). The effect vanishes when the height of the internal electron barrier at the interface, determined by cyclic voltammetry, becomes less than ≈0.4 eV. For low barrier thermally activated barrier crossing of electrons injected from either a Mg:Ag or an Al cathode prevails while at large barrier tunneling commences. It requires a critical potential drop across the interfacial layer, established by interfacial charging. While thermal barrier crossing is a monomolecular process independent of charging, tunneling involves a feedback process. The comparison between calculated and experimental response functions using barrier parameters determined by cyclovoltammetry is striking. The process could be exploited for fast switching of a LED. For that purpose a time scale of 100 ms as reported in [26] is inappropriate. However, the time response of the system is solely determined by the time by which the critical amount of charge is accumulated, i.e. by the injection efficiency of the electrodes and the charge carrier mobility.

CONCLUSION

By employing Monte-Carlo simulations and experiment a hopping concept has been formulated to understand charge carrier injection into a random organic dielectric which otherwise would be an

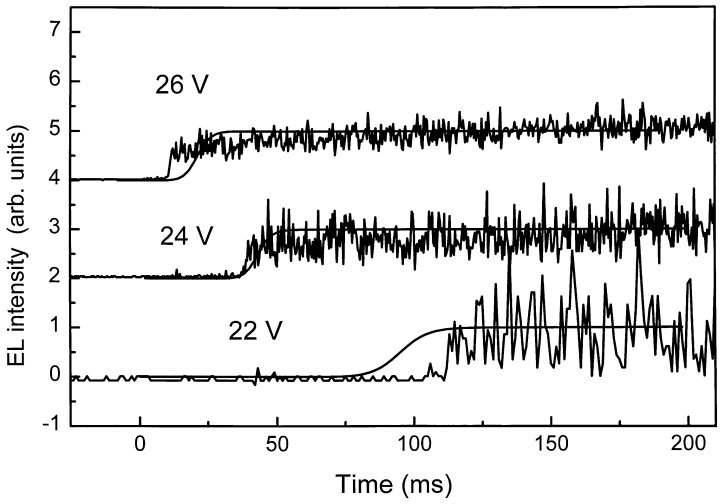

Fig. 11 Comparison between experimental (see [26]) and calculated (see [30]) EL traces from ITO|TSA:PSu|tert-butyl PQP|Mg multilayer LED at different applied voltages. The crucial parameters for the calculation are the energy barrier at the interface $H'_h = 1.3\,eV$ and $H'_0 = 0.65\,eV$.

insulator. Charge transport is usually disorder controlled. However, at weak energetic disorder it is controlled by poor electronic overlap between extended π-conjugated polymer segments. The transient behavior of bi-/multilayer LEDs turns out to be critically dependent on the height of internal energy barriers.

ACKNOWLEDGEMENT

We are grateful to Prof. H. H. Hörhold and Dr U. Scherf for placing conjugated polymers at our disposal. This work was supported by the *Deutsche Forschungsgemeinschaft* (*Sonderforschungsbereich 383 and 436 Rus 113/9314*) and the *Fond der Chemischen Industrie*.

REFERENCES

1 P. M. Borsenberger, D. Weiss. *Organic Photoreceptors for Imaging Systems*. Marcel Dekker, New York (1993).

2 N. Greenham, R. H. Friend. *Solid State Phys.* **49**, 1 (1995).

3 C. Weißmantel, C. Hamann. *Grundlagen der Festkörperphysik*. VEB Deutscher Verlag der Wissenschaften, Berlin (1981).

4 V. I. Arkhipov, E. V. Emelianova, Y. H. Tak, H. Bässler. *J. Appl. Phys.* **84**, 848 (1998).

5 U. Wolf, V. I. Arkhipov, H. Bässler. *Phys. Rev. B* **59**, 7507 (1999).

6 S. Barth, D. Hertel, Y. H. Tak, H. Bässler, H. H. Hörhold. *Chem. Phys. Lett.* **274**, 165 (1997).

7 S. Barth, U. Wolf, P. Müller, H. Riel, H. Vestweber, P. F. Seidler, W. Rieß, H. Bässler, submitted to *Phys. Rev. B*.

8 H. Ishii, K. Seki. *IEEE Transactions on Electron Devices* **44**, 1295 (1997).

9 P. W. M. Blom, M. J. M. de Jong, J. J. M. Vleggar. *Appl. Phys. Lett.* **68**, 3308 (1996).

10 M. A. Lampert, P. Mark. *Current Injection in Solids*. Academic Press, New York (1970).

11 L. S. Hung, C. W. Tang, M. G. Mason. *Appl. Phys. Lett.* **70**(2), 152 (1997).

12 D. M. Pai, J. F. Janus, M. Stolka. *J. Phys. Chem.* **88**, 4714 (1984).

13 O. L. Nelson, D. E. Anderson. *J. Appl. Phys.* **37**, 66 (1966).

14 U. Wolf, S. Barth, H. Bässler. *Appl. Phys. Lett.* **75**(14), 2035 (1999).

15 G. E. Jabbour, Y. Kawabe, S. E. Shaheen, J. F. Wang, M. M. Morrell, B. Kippelen, N. Peyghambarian. *Appl. Phys. Lett.* **71**(13), 1702 (1997).

16 H. Bässler. In *Primary Photoexcitons in Conjugated Polymers: Molecular Exciton versus Semiconductor Band Model* (N. S. Saviciftci, ed.), p. 51. World Scientific, Singapore (1998).

17 H. Bässler. *Phys. Stat. Sol. (b)* **175**, 15 (1993).

18 D. Hertel, H. Bässler, U. Scherf, H. H. Hörhold. *J. Chem. Phys.* **110**, 9214 (1999).

19 M. Pope, C. E. Swenberg. *Electronic Processes in Organic Crystals.* Clarendon Press, Oxford (1982).

20 B. Reimer, H. Bässler. *Phys. Stat. Sol. (b)* **85**, 145 (1978).

21 N. Fisher. *J. Phys. Condens. Matter* **4**, 2543 (1992).

22 A. S. Siddiqui, G. E. Wilson. *J. Phys. Chem.: Solid State Phys.* **12**, 4237 (1979).

23 J. Grimme, M. Kreyenschmidt, F. Uckert, K. Müllen, U. Scherf. *Adv. Mater.* **7**, 292 (1995).

24 H. Vestweber, R. Sander, A. Greiner, W. Heitz, R. F. Mahrt, H. Bässler. *Synth. Mett.* **64**, 141 (1994).

25 D. D. C. Bradley. *Synth. Met.* **64**, 401 (1993).

26 J. Pommerehne, H. Vestweber, W. Guss, R. F. Mahrt, H. Bässler, M. Porsch, J. Daub. *Adv. Mat.* **7**, 551 (1995).

27 D. V. Khramtchenkov, V. I. Arkhipov, H. Bässler. *J. Appl. Phys.* **81**, 6954 (1997).

28 V. R. Nikitenko, Y. H. Tak, H. Bässler. *J. Appl. Phys.* **84**, 2334 (1998).

29 J. Pommerehne, A. Selz, K. Book, F. Koch, U. Zimmermann, C. Unterlechner, J. H. Wendorff, W. Heitz, H. Bässler. *Macromolecules* **30**, 8270 (1997).

30 V. R. Nikitenko, H. Bässler. *J. Appl. Phys.* **85**, 6515 (1999).